

MODELLING THE HARDENABILITY AND TEMPERING OF HIGH STRENGTH STEELS

JOHAN ELIASSON¹, TADEUSZ SIWECKI¹, BJÖRN RODELL²

¹ Corrosion and Metals Research Institute, KIMAB
Drottning Kristinas väg 48, S-114 28 Stockholm, Sweden

² SSAB Oxelösund AB, Sweden

Abstract

The aim of the present work was to develop hardenability and tempering models for various quenching and tempering treatments of high strength /martensitic steels.

The hardenability model developed at KIMAB is divided in three sub-models: (i) Dissolution of particles during reheating, (ii) Calculation of hardenability distance kinetically depending on the dissolution of particles and (iii) Grain growth (includes the Zener pinning effect of size and volume fraction of the particles). The hardenability model calculates the Ideal Diameter, Jominy distance to 50% martensite and surface hardness of steel after quenching. Examples of the predictions on a steel from SSAB Oxelösund are presented here in the paper in comparison to the experimental data.

The tempering model was also developed at KIMAB as an empirical model, which has been based on experimental data from the literature. Hardness and ultimate tensile strength of a quenched steel, originated from Ovako Bar, after tempering in the temperature range 150°-700°C were calculated and the results were compared with the experimental data.

The tempering model generally functioned well and good agreement of predictions with experimental data has been obtained. However, the thermal history before quenching is important to take into consideration because this affects the level of hardness and strength. By applying the hardenability model together with the tempering model the effect of undissolved particles on the properties of tempered steels could be studied.

Key words: hardenability, carbide dissolution, modelling, tempering, grain growth, microalloyed steels

1. INTRODUCTION

The hardening process of modern high strength steels places new demands for accurate hardenability predictions. The complex matter of particle precipitation and microstructure development during processing makes it necessary to have an accurate kinetic hardenability model. The benefit of using the model for hardenability predictions is to reduce the costs for material development as well as production costs with improved properties of the final products.

The main goal for the steel industry is to reduce the number of Jominy tests and testing of the process parameters that will be carried out during development of new hardened steel grades, thereby reducing

costs in the development stage. Other important goals are tailoring of mechanical properties with respect to alloying of the steels and reduction of weight by usage of steels with higher strength.

In many cases steels are overalloyed to ensure full hardenability. This can however increase the cost of the steel with no beneficial gain in the mechanical properties. With the help of modelling overalloying should be avoided. So, the benefits of modelling are reduced costs for material development as well as production costs with improved properties of the final products.

The best known formalism for predicting hardenability was developed by Grossman in the early

nineteen-forty's (Grossman, 1942). According to his formalism, the ideal critical size, (DI), can be calculated using the following equation:

$$DI = D * MF1 * MF2 * \dots * MF_n \quad (1)$$

where: $MF1 * MF2 * \dots * MF_n$ are hardenability multiplying factors for the various alloying elements present in the steel and D is the critical size for the corresponding Fe-C-alloy.

The multiplying factors are assumed to be functions of the concentration of each specific element only.

The multiplying factors MF above, may be expressed as follows:

$$MF_i = (1 + f_i (\text{wt\% } M_i)) \quad (2)$$

where f_i are proportionality constants for the linear parts of the curves as shown in Figure 1, and M_i refers to a specific element.

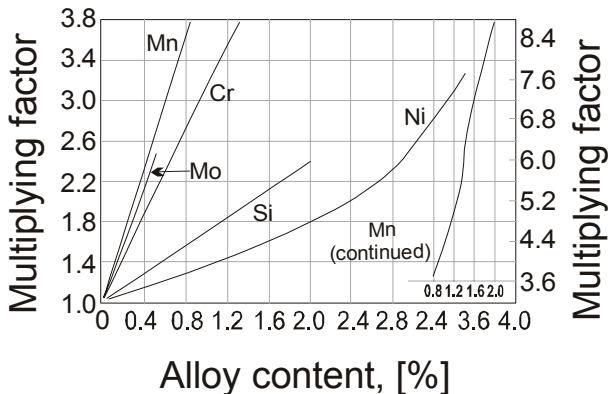


Fig. 1. Hardenability multiplying factors according to AISI (Grossman, 1942).

Due to its simplicity, the Grossman method has become the standard method for calculating hardenability throughout the world, although already in his original paper Grossman pointed out some limitations of the model. It has been found that the hardenability effect of microalloying elements, in particular, cannot be separated; there are combination effects. The precipitation behaviour gives rise to inconsistency when using the Grossman multiplying factors for predicting hardenability of modern microalloyed steels. A kinetic hardenability model must be able to predict the amounts of the elements that are in the form of particles and the amounts in solution in the austenite during quenching (Rodell and Siwecki, 2000).

The aim of the present work is to develop the hardenability and tempering models for various quenching and tempering treatments of high strength/martensitic steels.

2. DEVELOPMENT OF HARDENABILITY MODEL

Description of sub-models in the hardenability model is based on three phenomena that are modelled simultaneously in MATLAB: particle dissolution behaviour, grain growth during reheating and hardenability in relation to the Grossman Ideal Diameter. So, the model is divided in the following sub-models;

1. Particle Dissolution,
2. Grain Growth,
3. DI-Calculation.

The formation and reheat temperatures as well as the equilibrium amounts of the elements are input values for the three sub-models (Rodell and Siwecki, 2000).

2.1. Sub-model for Dissolution of Carbonitride Particles

The particle dissolution sub-model described below is a development of an earlier version for particle dissolution developed at KIMAB. The model described below calculates the dissolution of four multi-component particle types and is directed more specifically towards hardenability modelling; however both models can be used as sub-models in the program. The model is based upon an equation for dissolution of a spherical MCN particle in an infinite iron matrix (equation 3). The equation is solved simultaneously for all the substitutional elements in the steel. The radius change is described by

$$\frac{dr}{dt} = -\frac{\Omega D_M^\gamma}{r} \quad (3)$$

where; Ω is a measure of the driving force given by;

$$\Omega = \frac{x_M^{\gamma/MCN} - x_M^{\gamma\infty}}{x_M^{MCN/\gamma} - x_M^{\gamma/MCN}} \quad (4)$$

The initial composition for the particle, $x_M^{MCN/\gamma}$, and the initial concentration in the austenite, far away from the particle, $x_M^{\gamma\infty}$, are chosen from the equilibrium values at the formation temperature, e.g. 600°C. The concentration in the austenite in contact with the particle, $x_M^{\gamma/MCN}$, is chosen from a global equilibrium calculation at the dissolution (reheat) temperature. Amounts of the elements in particles and in austenite are continuously updated, changing $x_M^{MCN/\gamma}$ and $x_M^{\gamma\infty}$ values as the atoms move away from the particle to the austenite during the dissolution. In this way, the concentration gradient de-



creases. The transport of an element stops when the concentration of the element in the austenite, x_M^{∞} is equal to the global equilibrium concentration value in the austenite, $x_M^{\gamma/MCN}$.

All thermodynamic data are calculated using ThermoCalc software (www.thermocalc.se) together with a database for HSLA steels.

The precipitated elements are combined into four particle types based upon knowledge of their stability:

1. Low temperature dissolved particles (LTD) containing Fe, Mn, Si, Cu, Cr, Ni, B,
2. Mo, V carbonitride (MoV),
3. AlN particles (AlN),
4. Ti, Nb carbonitride (TiNb).

Initial radii for the four particle types are chosen manually. The radii of the four particles during dissolution depend on the transport of each element that it contains, from the matrix to the austenite. The four particle radii are input for the Grain growth sub-model. The amounts of the elements that are in solution in the austenite are constantly updated and serve as input for the D_1 calculation sub-model. At present, only one substitutional lattice is considered. The interstitial elements are not considered in the calculation.

2.2. Sub-model for Grain Growth during Reheating

Grain growth is simulated based upon the expression by Hillert (Hillman & Hillert, 1975)

$$\frac{dR_i}{dt} = M\gamma \left(\frac{1}{R_{cr}} - \frac{1}{R_i} \pm z_{ij} \right) \quad (5)$$

where R_i is the radius of grain i , M is the grain boundary mobility, γ is the grain boundary energy and z_{ij} is the Zener parameter. R_{cr} is the critical radius of a grain that neither grows nor shrinks in the distribution of grains. The Zener parameter describes the effect of particles inhibiting the grain boundary movement and should therefore be introduced with a minus sign for growing grains and a plus sign for shrinking grains. See previous work (Siwecki and Rodell, 2003) for further description.

2.3. Calculation of Steel Hardenability

Earlier studies (Rodell and Siwecki, 2000) have shown that in order to determine the hardenability of modern microalloyed steels, it is necessary to take into account the dissolution behaviour of the microalloying elements. Elements like niobium and alumin-

ium are neglected in the existing hardenability predictors even though they have a powerful hardenability increasing effect in solid solution (Grossman, 1942, Rodell and Siwecki, 2000). This promoted our new concept for the hardenability calculation: to separate the influence of elements in solution in the austenite from the precipitated elements.

The hardenability calculation is performed in a sub-model for calculating D_1 (Rodell and Siwecki, 2000). The model calculates Ideal Diameter (D_1), Jominy distance to 50% martensite (JD50) and surface hardness after quenching. The program calculates multiplying factors for (0-1.95) wt% Mn, (0-2 wt%) Si, (0-2 wt%) Ni, (0-1.75 wt%) Cr, (0-0.55 wt%) Mo, (0-0.55 wt%) Cu, (0-0.2 wt%) V, (0-0.1 wt%) Al, as well as the boron factor. The multiplying factors including the boron factor are calculated based upon equations in the ASTM standard (ASTM Standard A 255-95, 1995), whereas the multiplying factor for Al is based upon Grossman's original work (Grossman, 1942). The ideal diameter is calculated using equation 1.

The approach makes it possible to identify the combination effects of the alloying elements. It also lays the foundation for analysing the complex hardenability effects of particle forming elements such as Ti, Al, Nb, and V including boron protection. The concentration of the elements is calculated in the sub-model for particle dissolution.

At the present stage, the model uses equations based upon earlier experimental data, in which the combination effects become a part of the experimental error. New experiments are necessary to accurately determine multiplying factors for the new model.

Old multiplying factors may also be modified if there is detailed information about the steel compositions used for the determination of the equations.

3. DEVELOPMENT OF TEMPERING MODEL

The effects of alloying elements on hardness are given in the form of diagrams at different tempering temperatures in work by Grange et al., 1977. These diagrams were analysed and a Weibull type of relation was used to fit the influence of alloying elements on hardness. The results are presented in Eliasson's work (Eliasson and Siwecki, 2004). The following alloying elements are included in the model and affect the tempering behaviour: C, Si, Mn, Ni, Cr, Mo, V and P.

The calculations are first divided into a base hardness that predicts the hardness in a steel alloyed



only with carbon, and second the predicted additive effect on hardness from each alloying element.

The base hardness of the carbon steel can be described by equation 6:

$$HV = a - be^{-cx^d} \quad (6)$$

where a , b , c and d are constants and x is the carbon content in weight-%.

A similar type of relation is used for the additive effect on base hardness for each of the following alloying elements in the steel; Si, Mn, Cr, Ni, Mo, V and P.

$$\Delta HV_i = a_i - b_i e^{-c_i x_i^{d_i}} \quad (7)$$

where ΔHV_i is the increase in hardness in comparison with the hardness in a Fe-C steel as a function of added alloying element in weight-% in accordance with Grange's work (Grange et al., 1977).

Examples of the influence of the alloying element Mo on hardness after tempering for one hour at different temperatures are given in Figure 2. Equation 7 is applied to these curves and used during modelling. All coefficients for the elements at each tempering temperature can be found in Eliasson's work (Eliasson and Siwecki, 2004).

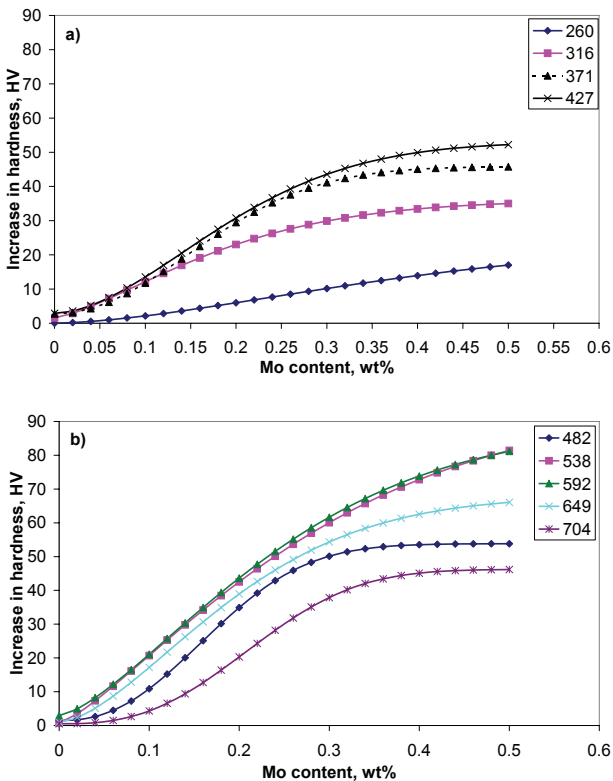


Fig. 2. Hardness increase vs. Mo-content after tempering for 1 h at temperatures, a) 260-427°C, b) 482-704°C.

4. MATERIALS USED FOR VERIFICATIONS OF HARDENABILITY AND TEMPERING MODELS

In this paper hardenability and tempering models are treated. The compositions of the steels studied are given in table 1.

Table 1. Approximate compositions of steels studied in this paper.

Steel	C	Si	Mn	Cr	Ni	Mo	V	Ti	Cu	Al	Nb	B	N
A	0.12	0.3	1.1	1	-	0.3	-	0.02	-	0.05	0.01	13	55
B	0.11	0.3	0.9	0.7	0.1	0.2	0.04	0.04	0.2	0.02	0.02	18	100

5. VERIFICATION EXAMPLE OF HARDENABILITY MODEL

In figure 3 hardenability is modelled for Steel A. The calculated Jominy distance is shown as a function of time. The estimated initial particle radii are given in the figure. During their dissolution into the austenite the hardenability increases. At higher temperature this process is faster. In this case the hardenability is over-estimated at higher austenitisation temperatures. The maximum hardenability is given as JDmax in the figure. This would be the value if all alloying elements were in solid solution before quenching, using

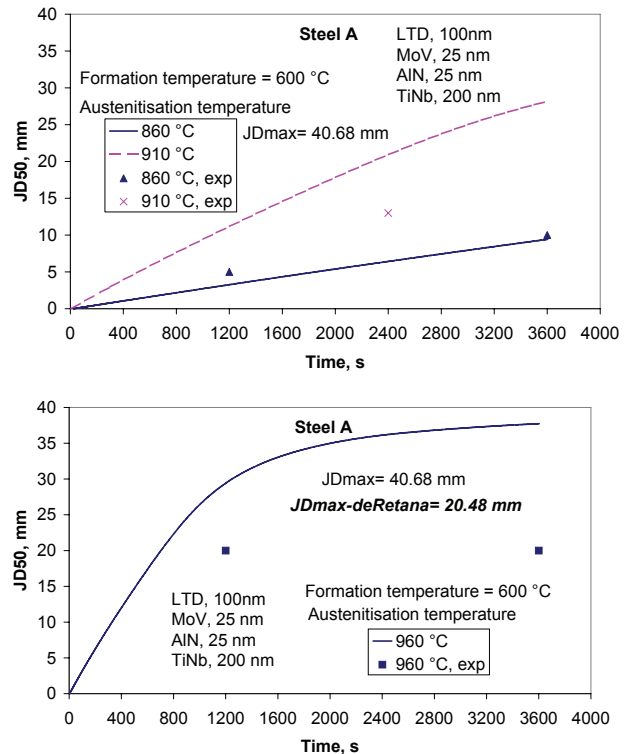


Fig. 3. Comparisons of calculated hardenability in Jominy distance (JD50) compared to experimental data as a function of time at different temperatures. Initial particle sizes are given.



Grossman hardenability factors. However, this concerns steel with low carbon content. According to reasearches (deRetana and Doane, 1971) the multiplications factors for e.g. Cr and Mo are reduced and contribute less to hardenability when the carbon content is below 0.2 wt-%. Also interaction effects such as those for Mo and Ni in low carbon steels occur. According to the literature a high Ni-content (>0.75 wt-%) increases the influence of Mo on hardenability. In figure 3 the JDmax value calculated with deRetana multiplying factors is given. This value is very close to the experimental value after austenitising at 960°C. So, it is the intention **to develop** the model in this direction considering both low carbon steels as well as steels with carbon contents above 0.2 wt-%. In table 2 the multiplication factors are given for steel A according to Grossmann and deRetana et al respectively. The combined multiplication factor for Cr and Mo is reduced with a factor 2 using the deRetana factors.

Table 2. Multiplication factors for Cr and Mo according to Grossmann (MG) and deRetana et al. (MR), and relation between the multiplication factors for Steel A.

	MG	MR	MG_{Cr*Mo}/MR_{Cr*Mo}
1 Cr	3.1	2.1	2
0.3 Mo	1.9	1.4	

6. VERIFICATION EXAMPLE OF TEMPERING MODEL

The chemical composition of the steel is given in the interface of the model in MATLAB. Then the tempering behaviour is calculated. Figure 4 shows the output results for Steel B. In the upper left figure the hardening contributions are shown as a function of tempering temperature. The base hardness due to carbon content is shown in the upper right figure. The total hardness is also given here. The ultimate tensile strength is calculated from hardness and is given in the lower left figure 4.

During modelling it was discovered that the decrease in hardness with tempering temperature on experimental data generally follows the decrease in the model. However, in many cases the experimental hardness is lower than the model predicted. The explanation for this is that (i) the steel is not fully hardened, and (ii) the particles are not full dissolved during austenitisation prior to hardening.

Therefore the tempering model was connected to the hardenability model. The calculated compositions of dissolved elements after hardening were then used as input in the tempering model.

In figure 5 this is described as follows: The fully hardened curve describes the hardness with the nominal composition of the steel. The following two curves are calculated after austenitisation at 1 h for 870 and 920°C. Not all of the alloying elements are then in solid solution before quenching. Approximate values are given in wt-% in the figure. By considering also the hardenability model the calculated hardness curve approaches the experimental curve for the steel.

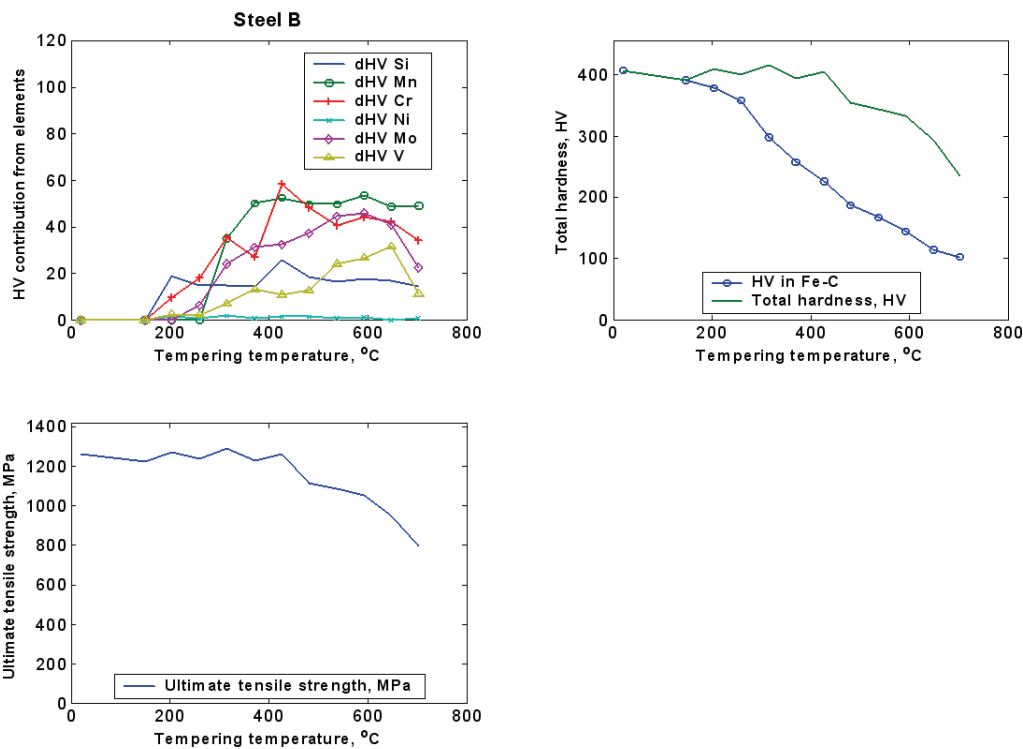


Fig. 4. Set of figures with output results from the tempering model in MATLAB describing HV contributions of elements, Total hardness and ultimate tensile strength as a function of tempering temperature.



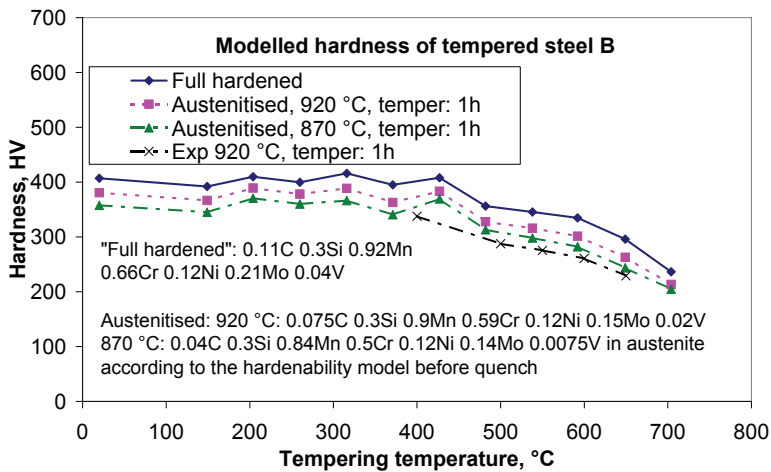


Fig. 5. Model predicted hardness in Vickers (HV) of tempered steel B as a function of tempering temperature.

7. SUMMARY

- The hardenability model, which includes three sub-models, is presented and discussed in this paper.
- The model considers important parameters such as dissolution of particles during reheat as well as grain growth that both affect hardenability of the steel with time. The output is steel hardenability in the form of Ideal Diameter based on Grossman hardenability factors for alloying elements, as well as Jominy Distance to 50% martensite and surface hardness.
- The hardenability model has been verified for the commercially processed steel from SSAB Oxelösund. It has concluded that the database used for prediction must be modified for steels with low carbon contents (for C-content lower than 0.12 wt-%).
- The tempering model developed for quenched high strength steel is also presented. Prediction of hardness and ultimate tensile strength of steel after tempering in the range 150°-700°C is considered.
- The tempering model has been also verified for the Ovako Bar steel. In the special case the hardness of steel was over-estimated, but the change in hardness with temperature is in accordance with the model. The lower hardness obtained in the calculation can be a result of undissolved particles before reheating.

- The hardenability model can be combined with the tempering model for prediction of hardness and strength properties of quenched and tempered steel. So, the effect of quenching temperature and time (undissolved particles) on the hardness/strength changes in the high strength steel can be studied in relation to the tempering parameters. The calculated hardness then approaches the experimental hardness of the studied steel.

Acknowledgements. Financial support from SSAB Oxelösund AB and Ovako Bar AB are gratefully acknowledged.

REFERENCES

- ASTM Standard A 255-95, 1995, *Standard Test Method for End-Quench Test for Hardenability of Steel*, 32-51.
- deRetana, A.F., Doane, D.V., 1971, Predicting the hardenability of carburizing steels, *Metal Progress*, 100, 65.
- Eliasson, J., Siwecki, T., 2004, Influence of alloying elements on mechanical properties in tempered martensitic steels, *Research report of Swedish Institute for Metals Research*, IM-2004-524.
- Grange, R.A., Hribal, C.R., Porter, L.F., 1977, Hardness of tempered martensite in carbon and low-alloy steels, *Met. Trans. A*, 8A, 1775-1785.
- Grossman, M.A., 1942, Hardenability calculated from chemical composition, *Trans. AIME*, 150, 227-229.
- Hillman, P., Hillert, M., 1975, On the effect of second-phase particles on grain growth, *Scand. J. Metall.* 4, 211-219
- Rodell, B., Siwecki, T., 2000, Hardenability model for steel: Part 1. Dissolution of particles, grain growth and ideal diameter, *Research report of Swedish Institute for Metals Research*, IM-2000-565
- Siwecki, T., Rodell, B., 2003, Modelling the effects of microalloying on the hardenability of high strength steels, *Symp. on the thermodynamics, kinetics, characterization and modelling of: austenite formation and decomposition*, Chicago, 227-245.
- www.thermocalc.se, *ThermoCalc Software*.

MODELOWANIE ZDOLNOŚCI DO HARTOWANIA I ODPUSZCZANIA STALI O PODWYŻSZONEJ

WYTRZYMAŁOŚCI

Streszczenie

Celem projektu jest opracowanie modeli hartowalności i odpuszczania dla różnych zabiegów obróbki cieplnej wysoko wytrzymałych stali martenzytycznych. Model hartowalności opracowany w KIMAB jest podzielony na trzy składowe: (i) Rozpuszczanie cząstek w czasie wygrzewania, (ii) Wyznaczenie obszarów zahartowanych w oparciu o kinetykę rozpuszczania cząstek i (iii) rozrost ziaren (uwzględniając wpływ rozmiaru i objętości cząstek na efekt piningu Zenera. Model hartowalności



przewiduje Idealną Średnicę, odległość Jominy'ego dla 50% martenzytu oraz twardość powierzchni stali po hartowaniu. Przykłady obliczeń dla stali z SSAB Oxelösund są przedstawione w artykule i porównane z wynikami doświadczeń.

W KIMAB opracowano również doświadczalny model odpuszczania, który opiera się na danych doświadczalnych zaczerpniętych z literatury. Obliczona została twardość i wytrzymałość na rozciąganie hartowanych stali, otrzymanych z Ovako Bar, po odpuszczeniu w temperaturach 150°-700°C, i wyniki porównano z pomiarami.

Model odpuszczania funkcjonuje poprawnie i ogólnie uzyskano zgodność z danymi doświadczalnymi. Niemniej jednak, historia zmian temperatury przed hartowaniem ma istotny wpływ i powinna być uwzględniona, ponieważ rzutuje ona na twardość i wytrzymałość stali. Stosując razem modele hartowności i odpuszczania można badać wpływ nierozpuszczonych cząstek na własności stali po obróbce cieplnej.

Submitted: September 18, 2006

Submitted in a revised form: November 23, 2006

Accepted: November 23, 2006

